Journal of Vacuum Science and Technology A

RESEARCH ARTICLE | MARCH 08 2023

NiO/β-$(Al_xGa_{1-x})_2O_3/Ga_2O_3$ heterojunction lateral rectifiers with reverse breakdown voltage >7 kV

Special Collection: Gallium Oxide Materials and Devices

Hsiao-Hsuan Wan ; Jian-Sian Li ; Chao-Ching Chiang ; Xinyi Xia ; Fan Ren ; Hannah N. Masten ; James Spencer Lundh ; Joseph A. Spencer ; Fikadu Alema ; Andrei Osinsky; Alan G. Jacobs ; Karl Hobart ; Marko J. Tadjer ; S. J. Pearton

J. Vac. Sci. Technol. A 41, 032701 (2023)
https://doi.org/10.1116/6.0002393

07 April 2024 10:55:47

NiO/β-$(Al_xGa_{1-x})_2O_3/Ga_2O_3$ heterojunction lateral rectifiers with reverse breakdown voltage >7 kV

Cite as: J. Vac. Sci. Technol. A **41**, 032701 (2023); doi: 10.1116/6.0002393
Submitted: 1 December 2022 · Accepted: 10 February 2023 ·
Published Online: 8 March 2023

View Online

Export Citation

CrossMark

Hsiao-Hsuan Wan,[1] Jian-Sian Li,[1] Chao-Ching Chiang,[1] Xinyi Xia,[1] Fan Ren,[1] Hannah N. Masten,[2] James Spencer Lundh,[2] Joseph A. Spencer,[2,3] Fikadu Alema,[4] Andrei Osinsky,[4] Alan G. Jacobs,[2] Karl Hobart,[2] Marko J. Tadjer,[2] and S. J. Pearton[5,a)]

AFFILIATIONS

[1]Department of Chemical Engineering, University of Florida, Gainesville, Florida 32611
[2]U.S. Naval Research Laboratory, Washington, DC 20375
[3]Virginia Tech, Blacksburg, Virginia 24060
[4]Agnitron Technology, Inc., Chanhassen, Minnesota 55317
[5]Department of Materials Science and Engineering, University of Florida, Gainesville, Florida 32611

Note: This paper is part of the Special Topic Collection on Gallium Oxide Materials and Devices.
[a)]**Electronic mail:** spear@mse.ufl.edu

07 April 2024 10:55:47

ABSTRACT

NiO/β-$(Al_xGa_{1-x})_2O_3/Ga_2O_3$ heterojunction lateral geometry rectifiers with diameter 50–100 μm exhibited maximum reverse breakdown voltages >7 kV, showing the advantage of increasing the bandgap using the β-$(Al_xGa_{1-x})_2O_3$ alloy. This Si-doped alloy layer was grown by metal organic chemical vapor deposition with an Al composition of ~21%. On-state resistances were in the range of 50–2180 Ω cm^2, leading to power figures-of-merit up to 0.72 MW cm^{-2}. The forward turn-on voltage was in the range of 2.3–2.5 V, with maximum on/off ratios >700 when switching from 5 V forward to reverse biases up to −100 V. Transmission line measurements showed the specific contact resistance was 0.12 Ω cm^2. The breakdown voltage is among the highest reported for any lateral geometry Ga_2O_3-based rectifier.

Published under an exclusive license by the AVS. https://doi.org/10.1116/6.0002393

I. INTRODUCTION

There is significant recent interest in the development of Ga_2O_3 power devices due to their capability for high temperature operation, reduced on-state and switching losses due to lower on-resistance for high voltage devices, and potentially higher frequency switching capability.[1–8] These are targeted for renewable energy transmission systems, electric vehicle (EV) traction inverter and motor control systems, fast charging stations, and more electric aircraft.[9,10] Since the efficiency of EV powertrain inverters is partially determined by the efficiency of the switching transistors, it is of interest to examine ultrawide-bandgap semiconductor electronics. The successful development of these power transistors is expected to significantly increase the longevity of a battery charge and the resultant cost of an EV. For devices in EV inverter applications, in addition to low switching loss and good thermal capability, high power and good robustness are highly desirable. In addition, the currently used passive and active filtering used to mitigate switching transients on motor drive systems in electro-hydrostatic and electromechanical actuators for air platforms could be replaced by optically gated power semiconductor devices.[11] The absence of a native p-type doping capability has led to the use of p-type oxides such as Cu_2O (Ref. 12) or NiO (Refs. 13–17) in heterojunctions with n-type Ga_2O_3.

An additional advance comes from the use of the wider bandgap alloy $(Al_xGa_{1-x})_2O_3$ in place of Ga_2O_3. $(Al_xGa_{1-x})_2O_3$ alloys with compositions up to $x = 40\%$ have been grown with good crystalline quality on (010)-oriented β-Ga_2O_3 substrates, and $x \geq 50\%$ can be obtained on (100) and (−201) β-Ga_2O_3 substrates when the layers are grown by metal organic chemical vapor deposition (MOCVD).[18–23] Phase pure β-$(Al_xGa_{1-x})_2O_3$ films with Al content up to 27% have been grown with this technique,[21–23] which is promising from the viewpoint that this is the standard epitaxial growth method for most compound semiconductors. While most Ga_2O_3-based rectifiers to date have been of vertical geometry to increase the current-carrying capability,[24–32] there is also interest

Published under an exclusive license by the AVS

in lateral geometry devices,[33] whose breakdown voltage can be more easily scaled by increasing the contact separation distance. Sundaram *et al.*[20] showed that the addition of a 30 nm-thick β-$(Al_{0.22}Ga_{0.78})_2O_3$ cap to an n-type β-Ga_2O_3 layer grown by metal organic chemical vapor deposition increased the breakdown voltage by ∼20%. The cap increased the surface Schottky barrier with Pt metal, resulting in reduced carrier injection under reverse bias. Masten *et al.*[19] reported β-$(Al_xGa_{1-x})_2O_3$/β-Ga_2O_3 heterostructure MESFETs with an on/off current ratio of ∼300 and a drain current of 1.8 mA/mm at a gate bias of 5 V and drain bias of 30 V.

In this paper, we demonstrate breakdown voltages >7 kV in lateral NiO/ β-$(Al_xGa_{1-x})_2O_3/Ga_2O_3$ heterojunction rectifiers, with the basic layer structure grown by MOCVD, with the bilayer NiO deposited by sputtering. The devices show promising on/off ratio and breakdown characteristics.

II. EXPERIMENT

The β-$(Al_xGa_{1-x})_2O_3$/β-Ga_2O_3 heterostructures were grown in an Agnitron Agilis 500 MOCVD reactor with trimethylaluminum (TMAl), triethylgallium (TEGa), and oxygen (5 N) as precursors and argon (6 N) as carrier gas.[19,20] The TMAl and TEGa precursors were used to grow 70 nm-thick Si-doped β-$(Al_xGa_{1-x})_2O_3$ layer on ∼300 nm UID β-Ga_2O_3 buffer layer, respectively, on a Fe doped (010) β-Ga_2O_3 1″ substrate (Synoptics). The AlGaO layer was Si doped using silane diluted in nitrogen (SiH_4/N_2) as the source with the targeted doping concentration of $\sim 4 \times 10^{17}$ cm^{-3}. The growth pressure was 15 Torr, and the growth temperature was 800 °C, while the oxygen flow rate for the growth of the AlGaO was 600 SCCM. The gas phase [TMAl]/([TMAl] + [TEGa]) molar flow rate ratio was ∼8.4%, producing an Al concentration of 20.6% calculated from x-ray diffraction (XRD). Room temperature Hall measurements showed a sheet resistance of $R_{SH} = 7636$ Ω/sq., with a sheet carrier concentration of 7.2×10^{12} cm^{-2} and associated electron mobility of 114 cm^2/V s. It should be noted that the unintentionally doped buffer is also somewhat conductive, around 10^{15} cm^{-3}, so the Hall measurements do not isolate the transport properties of the doped AlGaO layer. The Hall measurements were not corrected for any antiferromagnetic effects below the Neel temperature. We did not perform capacitance–voltage measurements due to the expected larger series resistance in the structure.

The NiO bilayer was deposited on top of the epi layer by magnetron sputtering from dual NiO targets at 3 mTorr and 150 W of 13.56 MHz power. The morphology of the layers deposited with the two targets was unchanged from those deposited with one target. We used two targets to increase the deposition rate to ∼0.2 Å s^{-1}. The Ar/O_2 gas ratio during sputtering was used to control the doping in the NiO in the range 2×10^{18}–2×10^{19} cm^{-3}, with mobility < 1 cm^2 V^{-1} s^{-1}, as determined by Hall measurements. We did not perform any corrections for the antiferromagnetic properties of NiO. This can only be done above the Neel temperature (∼525 K for NiO), at which thermal energy precludes spin moment alignment. At this temperature, there is a strong chance of altering the properties of the NiO. The bandgap was 3.8 eV, consistent with literature values.[34] We employed a bilayer of NiO of two different doping levels to both increase breakdown voltage and obtain low sheet resistance, as shown previously.[15] The band alignment for the NiO on Ga_2O_3 is type II, staggered gap, allowing facile transport of holes across the heterojunction.[35] Our preliminary results indicate this is still the case for NiO on the AGO, with the changes occurring mainly in the conduction band. The band alignment of NiO on AGO is expected to produce accumulation of electrons at the interface, i.e., 2DEG, owing to the large band offset at the conduction band.[36,37] The front-side of the device structure was contacted by 100 nm of Ni/Au metal, with circular contacts of 50–100 μm. Ohmic contacts to the lateral rectifier structure were made by 100 nm of Ti/Au. A schematic is shown in Fig. 1(a), while the different size rectifiers and the transmission line measurement (TLM) pattern used to extract contact resistance is shown in Fig. 1(b). The avoidance of a mesa etching process is an advantage of this technology.

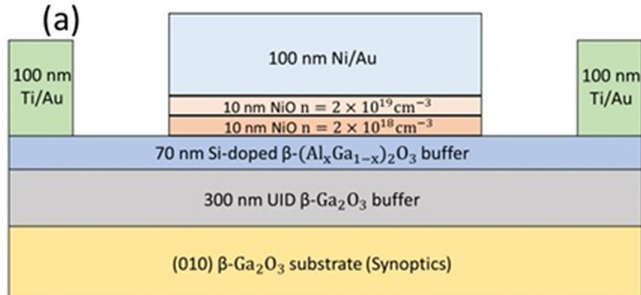

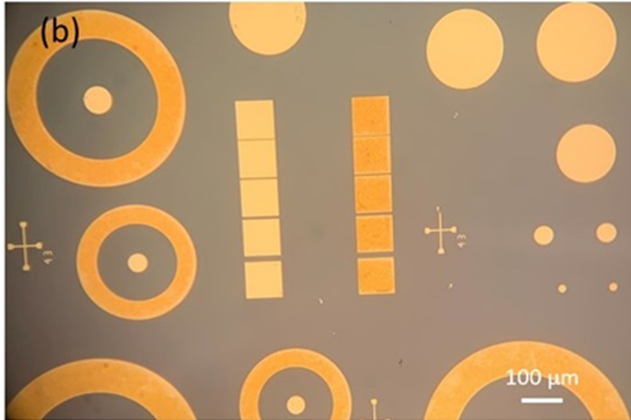

FIG. 1. (a) Schematic of lateral diode. (b) Optical image of diodes and contact metals for TLM measurement.

The current–voltage (*I–V*) characteristics at room temperature were recorded on a Tektronix 371-B curve tracer at high voltage while an Agilent 4156C was used for forward and reverse current measurements at low biases. Fits to thermionic emission were performed for forward bias conditions and for reverse voltages >300 V, fitting also performed for trap-assisted space-charge-limited current (SCLC). The reverse breakdown voltage was defined as the bias for a reverse current density reaching 1 A cm^{-2}.

III. RESULTS AND DISCUSSION

The TLM data for the structure are shown in Fig. 2. The specific contact resistance was 0.12 Ω cm^2, with a transfer length of

07 April 2024 10:55:47

Published under an exclusive license by the AVS

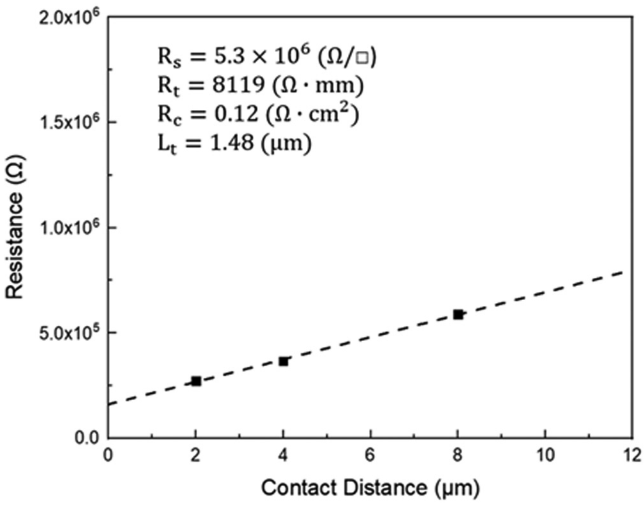

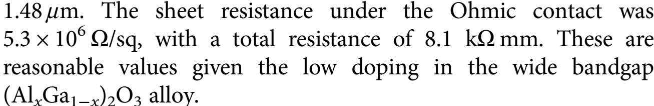
FIG. 2. TLM measurement data, showing the parameters extracted from the plot of resistance as a function of contact distance.

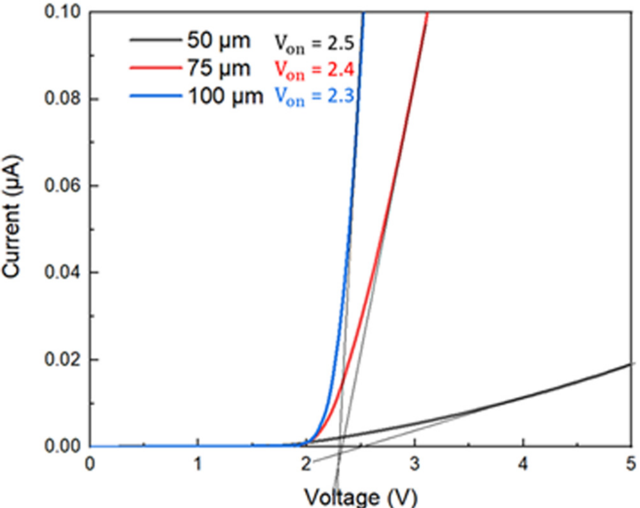

FIG. 4. Forward turn-on voltage for the three rectifier different diameters.

1.48 μm. The sheet resistance under the Ohmic contact was 5.3×10^6 Ω/sq, with a total resistance of 8.1 kΩ mm. These are reasonable values given the low doping in the wide bandgap $(Al_xGa_{1-x})_2O_3$ alloy.

Figure 3 shows the forward current density characteristics and associated on-state resistances, R_{ON}, for three different rectifier diameters. The power figure-of-merit (FOM), V_B^2/R_{ON}, where V_B is the reverse breakdown voltage, for the 50 μm rectifier was 0.01 MW cm^{-2}, for 75 μm was 0.34 MW cm^{-2}, while for 100 μm, FOM was 0.72 MW cm^{-2}. These are well below the values for vertical geometry NiO/Ga_2O_3 rectifiers because of the higher on-state resistance in lateral devices.[14–16] The forward current was still dominated by thermionic emission current.

Figure 4 shows linear plots of forward current to extract the forward turn-on voltage. This was in the range 2.3–2.5, consistent with previous reports for NiO/Ga_2O_3 rectifiers and demonstrating that the inclusion of the alloy did not degrade the turn-on voltage to a significant degree.[15–17]

The breakdown voltages were extracted from the reverse *I*–*V* characteristics, as shown in Fig. 5. The maximum value we obtained was over 7 kV. This is the highest reported value for a

07 April 2024 10:55:47

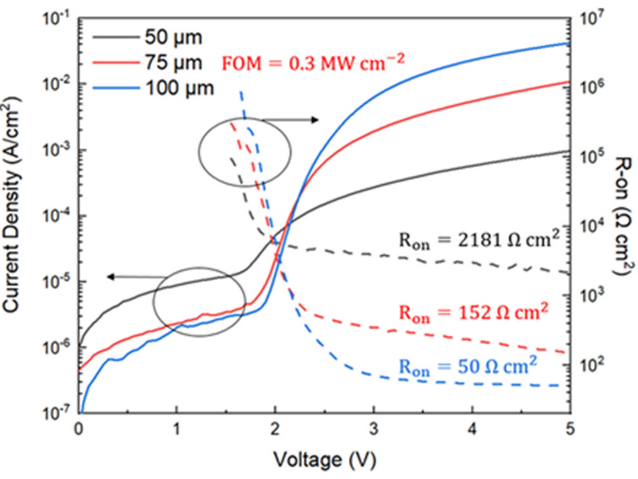

FIG. 3. Forward current density and on-state resistance for rectifiers of three different diameters.

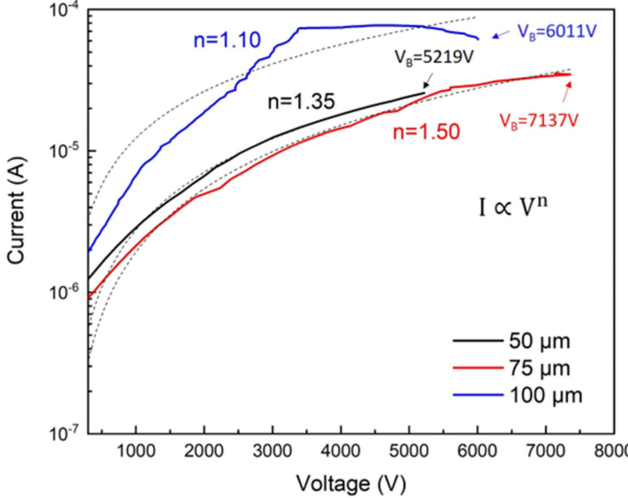

FIG. 5. Reverse *I*–*V* characteristics of rectifiers of three different diameters, showing the associated breakdown voltages.

Published under an exclusive license by the AVS

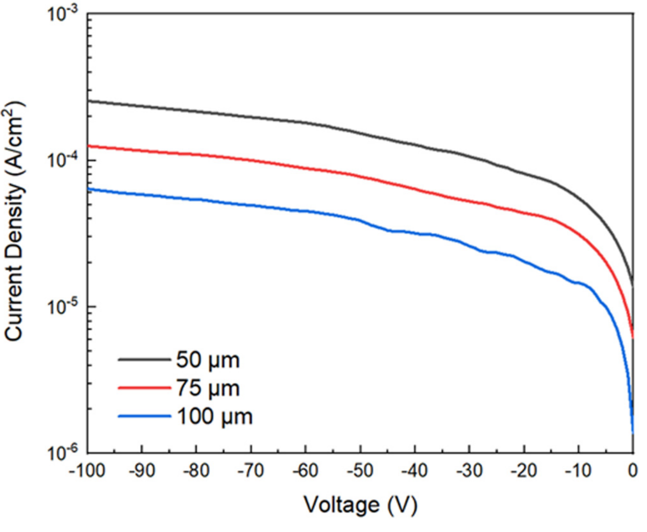

FIG. 6. Reverse *I*–*V* characteristics at low biases.

lateral Ga_2O_3 rectifier. Bhattacharya *et al.*[38] reported 4.4 kV breakdown in Ga_2O_3 metal semiconductor (MESFETs), while values <4 kV are reported for MESFETs and MOSFETs.[39–41] The highest breakdown voltage for a lateral MOSFET is 8.56 kV for 60 μm gate-drain separation, obtained after vacuum annealing and slightly higher than unannealed devices.[42,43] Note that the currents sharply increased above the breakdown voltages indicated in the figure, producing permanent degradation. The trap-filling conduction also led to plateaus in some of the *I*–Vs.

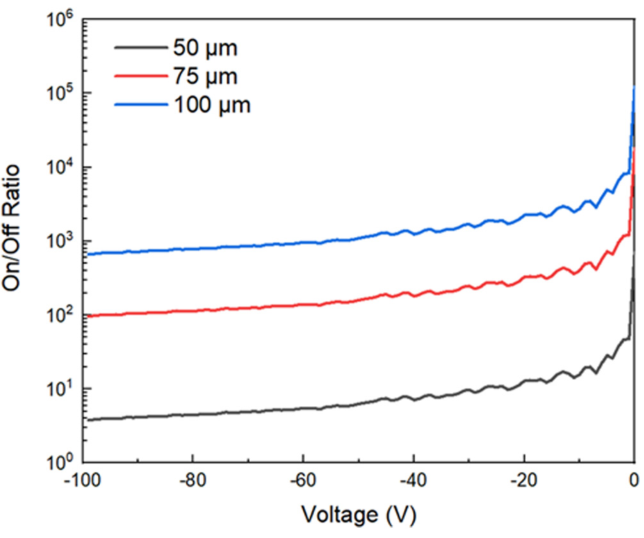

FIG. 7. On/off ratio when switching from +5 V to the value shown on the *x* axis for three different diameter rectifiers.

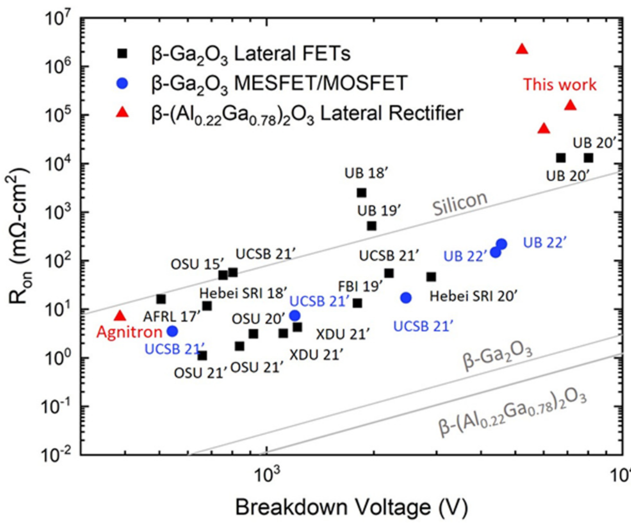

FIG. 8. Compilation of reported $R_{on,sp} - V_{BR}$ values for lateral geometry Ga_2O_3-based devices. The previously reported values come from Refs. 40–44.

A more detailed view of the reverse current at low biases, up to −100 V, is shown in Fig. 6. This reverse leakage current was dominated by thermionic field emission (TFE) in this bias range. At >~300 V, electron injection into the drift region produced an $I \propto V^n$ relationship, where $n < 2$. This is typical of trap-assisted space-charge-limited conduction.

Figure 7 shows the diode on–off ratio for the NiO/Ga_2O_3 heterojunction rectifiers when switching from +5 V forward voltage to reverse voltages shown on the *x* axis, i.e., up to −100 V. The maximum on/off ratio was >700.

To put the results in context, Fig. 8 shows a compilation of reported breakdown voltages and on-state resistances from different institutions.[40–44] The device types are mainly either MESFETs or various types of MOSFET geometries, which we have included under the general heading of lateral FETs. Our results show the advantage of both the ternary alloy to increase bandgap and the use of the NiO-$(Al_{0.21}Ga_{0.79})_2O_3$ p–n heterojunction. Since both switching devices and rectifiers are needed for inverter systems, it is worth developing both lateral and vertical geometry devices in this ultrawide bandgap materials system. The clear need is to lower the on-state resistance, while retaining the high breakdown voltages in our devices. Note that all of the reported figures-of-merit for lateral devices fall well short of the theoretical values for Ga_2O_3, with only some being superior at this stage to the limits for Si. This emphasizes how much more development is needed for Ga_2O_3 power electronics.

IV. SUMMARY AND CONCLUSIONS

Promising performance from NiO/β-$(Al_xGa_{1-x})_2O_3$/Ga_2O_3 heterojunction lateral geometry rectifiers was obtained, with maximum reverse breakdown voltage >7 kV. This is the highest reported for lateral rectifiers and shows the value of both the NiO

07 April 2024 10:55:47

Published under an exclusive license by the AVS

gate structure and the inclusion of the wider bandgap of the β-$(Al_xGa_{1-x})_2O_3$ alloy. It is not expected that there is significant leakage conduction contribution from the NiO layer due to formation of polarons in this material,[45–48] making this a good choice as the p-side of the heterojunction. However, although the breakdown voltage is quite high, the R_{ON} is extremely high as well in this lateral structure. Similar lateral GaN-based Schottky Barrier Diodes (SBDs) with a 2DEG channel have also been developed with the BV over 10kV. The latter is dependent on the separation of the electrodes. The current results are not competitive when compared with the GaN-based lateral SBD and indicate that much optimization is needed on solving the resistance issue. The high R_{ON} values mean the device performance is far from the AlGaO limit, with the R_{ON} values inferior to the projected Si limit. This is an area that must be optimized. The use of the industry standard MOCVD growth, simple fabrication, and avoidance of mesa etching processes are all advantages of the approach outlined in this work.

ACKNOWLEDGMENTS

Work was performed as part of Interaction of Ionizing Radiation with Matter University Research Alliance (IIRM-URA), sponsored by the Department of the Defense, Defense Threat Reduction Agency under Award No. HDTRA1-20-2-0002. The content of the information does not necessarily reflect the position or the policy of the federal government, and no official endorsement should be inferred. The work was also supported by NSF (No. DMR 1856662) (James Edgar). The authors thank the staff of the Nanoscale Research Facility at UF, part of the Herbert Wertheim College of Engineering's Research Service Centers (RSC), for their assistance in device fabrication. H.N.M. and J.-S.L. acknowledge postdoctoral funding from the National Research Council, Washington, DC. Fabrication equipment and support was provided by the NRL Nanoscience Institute and Brian Downey (NRL). The authors acknowledge John Blevins (AFRL) for providing Ga_2O_3 substrates for this work. Agnitron's ongoing β-Ga_2O_3 development work is in part supported by ONR (Contract No. N6833518C0192), under the direction of Lynn Petersen, and AFOSR (Contract No. FA9550-17-P-0029), under the direction of Ali Sayir. Research at the Naval Research Laboratory was supported by the Office of Naval Research.

AUTHOR DECLARATIONS

Conflicts of Interest

The authors have no conflicts to disclose.

Author Contributions

Hsiao-Hsuan Wan: Data curation (equal); Formal analysis (equal); Investigation (equal); Methodology (equal); Writing – original draft (equal). **Jian-Sian Li:** Data curation (equal); Formal analysis (equal); Investigation (equal); Methodology (equal); Writing – original draft (equal). **Chao-Ching Chiang:** Data curation (equal); Formal analysis (equal); Investigation (equal); Methodology (equal); Writing – original draft (equal). **Xinyi Xia:** Data curation (equal); Formal analysis (equal); Investigation (equal); Methodology (equal); Writing – original draft (equal). **Fan Ren:** Conceptualization (equal); Data curation (equal); Funding acquisition (equal); Writing – original draft (equal). **Hannah N. Masten:** Data curation (equal); Investigation (equal); Methodology (equal); Writing – original draft (equal). **James Spencer Lundh:** Data curation (equal); Formal analysis (equal); Investigation (equal); Methodology (equal); Writing – original draft (equal). **Joseph A. Spencer:** Data curation (equal); Formal analysis (equal); Investigation (equal); Methodology (equal); Writing – original draft (equal). **Fikadu Alema:** Conceptualization (equal); Data curation (equal); Formal analysis (equal); Funding acquisition (equal); Investigation (equal); Methodology (equal); Writing – original draft (equal). **Andrei Osinsky:** Conceptualization (equal); Data curation (equal); Formal analysis (equal); Funding acquisition (equal); Investigation (equal); Methodology (equal); Writing – original draft (equal). **Alan G. Jacobs:** Data curation (equal); Investigation (equal); Methodology (equal); Writing – original draft (equal). **Karl Hobart:** Conceptualization (equal); Funding acquisition (equal); Writing – original draft (equal). **Marko J. Tadjer:** Conceptualization (equal); Data curation (equal); Formal analysis (equal); Funding acquisition (equal); Writing – original draft (equal). **S. J. Pearton:** Data curation (equal); Investigation (equal); Methodology (equal); Writing – original draft (equal).

DATA AVAILABILITY

The data that support the findings of this study are available within the article.

REFERENCES

[1] M. Tadjer, Science **378**, 6621 (2022).
[2] S. J. Pearton, J. Yang, P. H. Cary IV, F. Ren, J. Kim, M. J. Tadjer, and M. A. Mastro, Appl. Phys. Rev. **5**, 011301 (2018).
[3] P. Dong, J. Zhang, Q. Yan, Z. Liu, P. Ma, H. Zhou, and Y. Hao, IEEE Electron. Device Lett. **43**, 765 (2022).
[4] E. Chikoidze *et al.*, J. Mater. Chem. C **7**, 10231 (2019).
[5] Y. Wang *et al.*, IEEE Trans. Power Electron. **37**, 3743 (2022).
[6] E. Ahmadi and Y. Oshima, J. Appl. Phys. **126**, 160901 (2019).
[7] S. J. Pearton, F. Ren, M. Tadjer, and J. Kim, J. Appl. Phys. **124**, 222901 (2018).
[8] J. Zhang *et al.*, Nat. Commun. **13**, 3900 (2022).
[9] A. J. Wileman, S. Aslam, and S. Perinpanayagam, Prog. Aerosp. Sci. **127**, 100739 (2021).
[10] J. Wang, IEEE Power Electron. Mater. **9**, 16 (2022).
[11] J. S. Sullivan, "Wide bandgap extrinsic photoconductive switches," Lawrence Livermore National Laboratory Report LL LLNL-TH-523591, 2012.
[12] T. Watahiki, Y. Yuda, A. Furukawa, M. Yamamuka, Y. Takiguchi, and S. Miyajima, Appl. Phys. Lett. **111**, 222104 (2017).
[13] J. Zhang *et al.*, ACS Appl. Electron. Mater. **2**, 456 (2020).
[14] Y. Lv *et al.*, IEEE Trans. Power Electron. **36**, 6179 (2021).
[15] H. H. Gong, X. H. Chen, Y. Xu, F.-F. Ren, S. L. Gu, and J. D. Ye, Appl. Phys. Lett. **117**, 022104 (2020).
[16] F. Zhou *et al.*, IEEE Trans. Power Electron. **37**, 1223 (2022).
[17] J.-S. Li, C.-C. Chiang, X. Xia, F. Ren, H. Kim, and S. J. Pearton, Appl. Phys. Lett. **121**, 042105 (2022).
[18] A. F. M. A. U. Bhuiyan, Z. Feng, J. M. Johnson, Z. Chen, H. Huang, J. Hwang, and H. Zhao, Appl. Phys. Lett. **115**, 120602 (2019).
[19] Hannah N. Masten, James Spencer Lundh, Joseph A. Spencer, Fikadu Alema, Andrei Osinsky, Alan G. Jacobs, Karl D. Hobart, and Marko J. Tadjer, paper presented at IWGO 2022, Japan, 20 October 2022.
[20] P. P. Sundaram, F. Alema, A. Osinsky, and S. J. Koester, J. Vac. Sci. Technol. A **40**, 043211 (2022).

07 April 2024 10:55:47

Published under an exclusive license by the AVS

[21]A. F. M. A. U. Bhuiyan, Z. Feng, H. Huang, L. Meng, J. Hwang, and H. Zhao, J. Vac. Sci. Technol. A **39**, 063207 (2021).
[22]A. F. M. A. U. Bhuiyan, Z. Feng, J. M. Johnson, H. Huang, J. Hwang, and H. Zhao, Appl. Phys. Lett. **117**, 142107 (2020).
[23]G. Seryogin, F. Alema, N. Valente, H. Fu, E. Steinbrunner, A. T. Neal, S. Mou, A. Fine, and A. Osinsky, Appl. Phys. Lett. **117**, 262101 (2020).
[24]K. Konishi, K. Goto, H. Murakami, Y. Kumagai, A. Kuramata, S. Yamakoshi, and M. Higashiwaki, Appl. Phys. Lett. **110**, 103506 (2017).
[25]K. Sasaki, D. Wakimoto, Q. T. Thieu, Y. Koishikawa, A. Kuramata, M. Higashiwaki, and S. Yamakoshi, IEEE Electron. Device Lett. **38**, 783 (2017).
[26]J. Yang, F. Ren, M. Tadjer, S. J. Pearton, and A. Kuramata, ECS J. Solid State Sci. Technol. **7**, Q92 (2018).
[27]J. Yang, F. Ren, Y. T. Chen, Y. T. Liao, C. W. Chang, J. Lin, M. J. Tadjer, S. J. Pearton, and A. Kuramata, IEEE J. Electron. Devices **7**, 57 (2019).
[28]Z. Hu, H. Zhou, K. Dang, Y. Z. Cai Feng, Y. Gao, Q. Feng, J. Zhang, and Y. Hao, IEEE J. Electron Devices **6**, 815 (2018).
[29]C. Joishi, S. Rafique, Z. Xia, L. Han, S. Krishnamoorthy, Y. Zhang, S. Lodha, H. Zhao, and S. Rajan, Appl. Phys. Express **11**, 031101 (2018).
[30]W. Li, K. Nomoto, Z. Hu, D. Jena, and H. G. Xing, IEEE Electron. Device Lett. **41**, 107 (2020).
[31]M. Ji, N. R. Taylo, I. Kravchenko, P. Joshi, T. Aytug, L. R. Cao, and M. Parans Paranthaman, IEEE Trans. Power Electron. **36**, 41 (2021).
[32]Ming Xiao *et al.*, IEEE Trans. Power Electron. **36**, 8565 (2021).
[33]W. Xiong *et al.*, IEEE Electron. Device Lett. **42**, 430 (2021).
[34]J. A. Spencer, A. L. Mock, A. G. Jacobs, M. Schubert, Y. Zhang, and M. J. Tadjer, Appl. Phys. Rev. **9**, 011315 (2022).
[35]X. Xia, J. S. Li, C. C. Chiang, T. J. Yoo, F. Ren, H. Kim, and S. J. Pearton, J. Phys. D: Appl. Phys. **55**, 385105 (2022).
[36]X. Lu, X. Zhou, H. Jiang, K. W. Ng, Z. Chen, Y. Pei, K. M. Lau, and G. Wang, IEEE Electron. Device Lett. **41**, 449 (2020).
[37]H. Gong, X. Chen, Y. Xu, Y. Chen, F. Ren, B. Liu, S. Gu, R. Zhang, and J. Ye, IEEE Trans. Electron. Devices **67**, 3341 (2020).
[38]A. Bhattacharyya *et al.*, Appl. Phys. Express **15**, 061001 (2022).
[39]Y. Lv *et al.*, IEEE Electron. Device Lett. **41**, 537 (2020).
[40]A. Bhattacharyya, P. Ranga, S. Roy, C. Peterson, F. Alema, G. Seryogin, A. Osinsky, and S. Krishnamoorthy, IEEE Electron. Device Lett. **42**, 1272 (2021).
[41]K. Zeng, A, Vaidya, and U. Singisetti, IEEE Electron. Device Lett. **39**, 1385 (2018).
[42]S. Sharma, L. Meng, A. F. M. Anhar Uddin Bhuiyan, Z. Feng, D. Eason, H. Zhao, and U. Singisetti, IEEE Electron. Device Lett. **43**, 2029 (2022).
[43]S. Sharma, K. Zeng, S. Saha, and U. Singisetti, IEEE Electron. Device Lett. **41**, 836 (2020).
[44]K. Tetzner *et al.*, IEEE Electron. Device Lett. **40**, 1503 (2019).
[45]R. Karsthof, M. Grundmann, A. M. Anton, and F. Kremer, Phys. Rev. B **99**, 235201 (2019).
[46]G. Geneste, B. Amadon, M. Torrent, and G. Dezanneau, Phys. Rev. B **96**, 134123 (2017).
[47]K. Jung, H. Seo, Y. Kim, H. Im, J. Hong, J.-W. Park, and J.-K. Lee, Appl. Phys. Lett. **90**, 052104 (2007).
[48]Y.-H. Hong *et al.*, Appl. Phys. Lett. **121**, 212102 (2022).

07 April 2024 10:55:47

Published under an exclusive license by the AVS